



This open access document is published as a preprint in the Beilstein Archives with doi: 10.3762/bxiv.2019.19.v1 and is considered to be an early communication for feedback before peer review. Before citing this document, please check if a final, peer-reviewed version has been published in the Beilstein Journal of Organic Chemistry.

This document is not formatted, has not undergone copyediting or typesetting, and may contain errors, unsubstantiated scientific claims or preliminary data.

Preprint Title Host–guest interactions in *nor-seco-cucurbit*[10]uril: novel guest-dependent molecular recognition and stereoisomerism

Authors Xiaodong Zhang, Wei Wu, Zhu Tao and Xin-Long Ni

Article Type Full Research Paper

Supporting Information File 1 supporting information.doc; 1.2 MB

ORCID® iDs Xin-Long Ni - <https://orcid.org/0000-0002-5557-1631>

Host–guest interactions in *nor-seco-cucurbit*[10]uril: novel guest-dependent molecular recognition and stereoisomerism

Xiaodong Zhang, Wei Wu, Zhu Tao, and Xin-Long Ni*

Key Laboratory of Macrocyclic and Supramolecular Chemistry of Guizhou Province,
Guizhou University, Guiyang 550025, China.

Email: X.-L. Ni* - longni333@163.com

* Corresponding author

Abstract

The unique monomer and excimer fluorescence emissions of pyrene were first exploited as distinctly photophysical signals to identify the possible diastereomers of guests within *nor-seco-cucurbit*[10]uril (NS-CB[10]) cavities. Further experiments revealed that balancing the hydrophilic and hydrophobic effects of the guest in aqueous solution can improve the molecular recognition and binding ability of NS-CB[10].

Keywords

nor-seco-cucurbit[10]uril; Host-guest interaction; Pyrene; fluorescent; molecular recognition

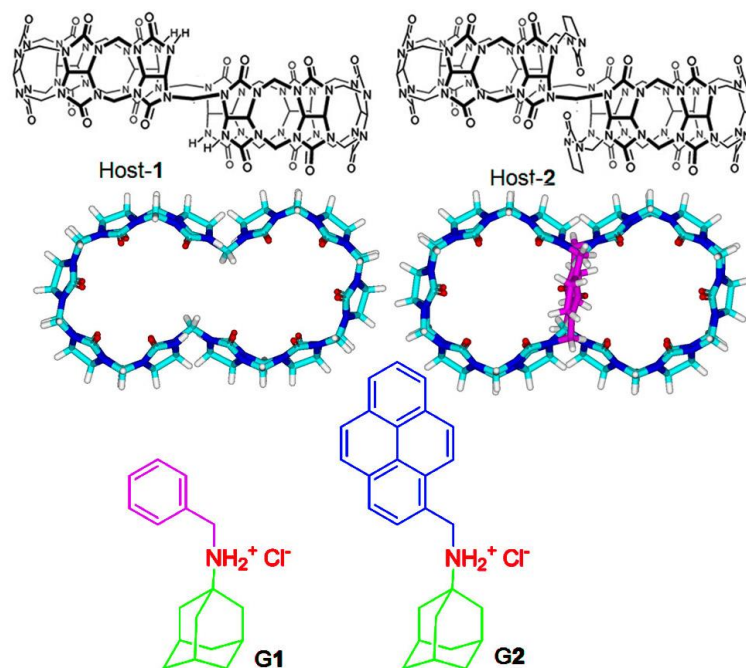
Introduction

Host–guest interactions that trigger molecular recognition are a current topic of interest. For example, understanding the protein–ligand molecular recognition is of paramount importance in the study of enzymatic catalysis and allosteric regulation of cell signaling, as well as in the design of efficient drugs that utilize host–guest interaction [1]. Cucurbit[*n*]urils (Q[*n*]s or CB[*n*]s) [2,3] having been viewed to have high potential use in host–guest chemistry in aqueous solution because of their varying cavity rigidity and larger portal sizes as compared with those of other macrocyclic hosts [4,5]. For example, cucurbit[8]uril (Q[8] or CB[8]), a large homologue of the Q[*n*] family, is unique because of its ability to bind two hetero- and homo-aromatic guests in its cavity through host-stabilized charge-transfer or π – π interactions [6]. This novel property of Q[8] has been utilized as molecular container for biological substrates [7], as well as in the construction of various supramolecular assemblies with specific structures and properties [8]. However, forming ternary complexes with Q[8] is challenging because of the number of aromatic-derived water-soluble recognition motifs remains limited.

In 2006, Isaacs and co-workers reported the synthesis and isolation of *nor*-secocucurbit[10]uril (NS-CB[10], host-1, Scheme 1) [9], a new member of the extended Q[*n*] family that contains two identical cavities. Different from the Q[8] host, NS-CB[10] can not only accommodate two aromatic guest molecules such as MV, but also has the ability to accommodate two other guest molecules such as adamantaneammonium (ADA) or alkylammonium ions into the cavity, forming a ternary complex. The novel binding capacity of NS-CB[10] has been utilized to form supramolecular polymers [10] and polymer nanoparticles [11]. More importantly, Isaacs et al. discovered that when the unsymmetrical guest ADA molecules are bound within NS-CB[10], three diastereomers such as top–top, center–center, and top–center can be observed. These diastereomers display homotropic allostery based on a guest-size-induced preorganization mechanism [9]. However, the same ADA guest was not incorporated into the cavity after NS-CB[10] was functionalized with imidazolidone (host-2, Scheme 1) [12].

Herein, we report the supramolecular host–guest interactions of the two cavities of NS-CB[10]-based host-1 and host-2 with two unsymmetrical ADA-based derivatives (G1 and G2, Scheme 1). As expected, hosts-1 and -2 are

capable of simultaneously binding guest G1, thus forming 1:2 ternary complexes by including different groups of G1 into the cavity. For example, host-1 can accommodate the ADA moiety into the cavity, whereas host-2 tends to include the benzyl group into the cavity. This behavior may be attributed to the bridging imidazolidone units of host-2 that rigidify its structure and make it selective toward smaller guests. However, we found that the ADA group can be accommodated into the cavity of host-2 when a larger hydrophobic unit such as pyrene instead of a benzyl group was appended to the ADA scaffold (G2). Interestingly, the top–center isomerism of G2 within both of hosts-1 and 2 could characterize because of the novel monomer and excimer photophysical property of pyrene as fluorophore. As a result, we demonstrated here a novel guest-controlled molecular recognition and stereoisomerism for the first time.



Scheme 1 Chemical structures of host-1, host-2, G1, and G2.

Results and Discussion

We took advantage of the two novel identical cavities and the simple formation of ternary diastereomers complex with NS-CB[10]-based hosts-1 and -2. The size of each cavity of host-1 is similar in size to Q[7], and the cavity size of host-2 is close to that of Q[6]. We first designed and prepared the ADA–benzyl-based ammonium guest molecules G1. We synthesized this compound because ADA can form a highly

stable complex with Q[7] (the highest reported K value for the ADA-Q[7] complex is 10^{12} M^{-1}) [13]; while benzyl ammonium ions can be included in both of cavities of Q[7] and Q[6]. Figure 1 shows the ^1H NMR spectral changes of the G1 guest in D_2O ($\text{pD} = 2.0$) in the presence of host-1 at different concentrations. Upon gradual addition of host-1 (0–0.4 equiv) to the solution of G1, the resonances corresponding to the protons on G1 split into two sets of signals. For example, one shifted upfield (ADA moiety) or downfield (benzyl moiety), and one remained at the original position. This result may be attributed to the slow movements of complexed and uncomplexed forms of G1 with host-1 on the NMR time scale; therefore, free G1 and the G1·host-1 complex were individually observed. With increasing concentrations of host-1 to ~0.5 equiv (Figure 1), the original proton signal disappeared. In particular, the peak of the protons on the ADA moiety shifted upfield from δ 2.23–1.65 ppm to δ 1.60–1.09 ppm, whereas the signals for the protons on the benzyl group substantially shifted downfield from δ 7.44 ppm to 7.48, 7.65, 7.89, and 8.38 ppm. These results suggest that host-1 cavities encapsulated the ADA moiety of G1 (upfield shift due to the shielding effect of the hydrophobic cavity) and that the benzyl group was on or near the host-1 portal (downfield shift due to the deshielding effect of the carbonyl-rimmed portal). Isothermal titration calorimetry results reveal a 2:1 G1/host-1 stoichiometry with a binding constant (K_a) of $1.32 \times 10^5 \text{ M}^{-1}$ (Table 1). These observations clearly indicate that host-1 recognizes and prefers to include the ADA moieties in both of the identical cavities with homotropic allosteric effect.

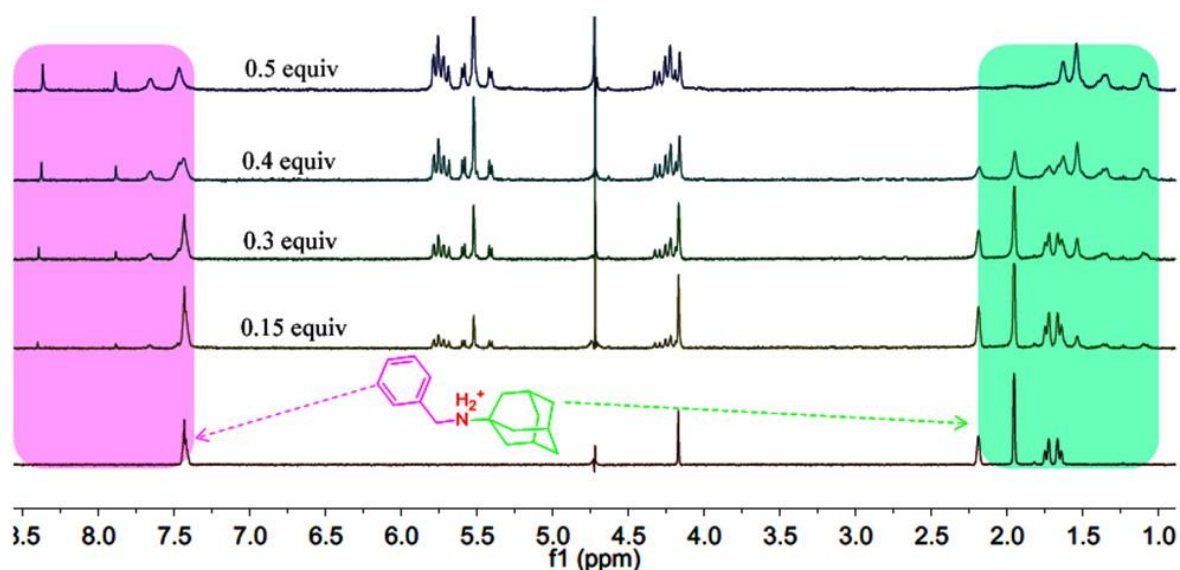


Figure 1 ^1H NMR spectra of G1 (1.0 mmol, D_2O , $\text{pD} = 2.0$) in the presence of host-1 at different concentrations at 298K.

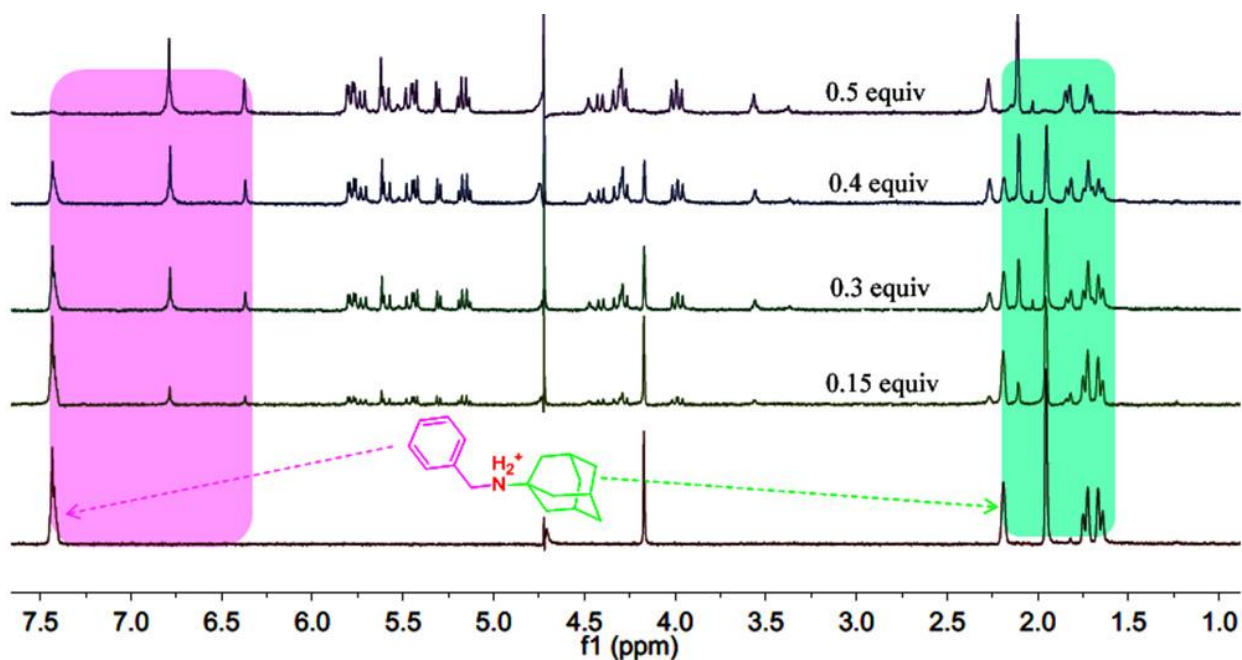


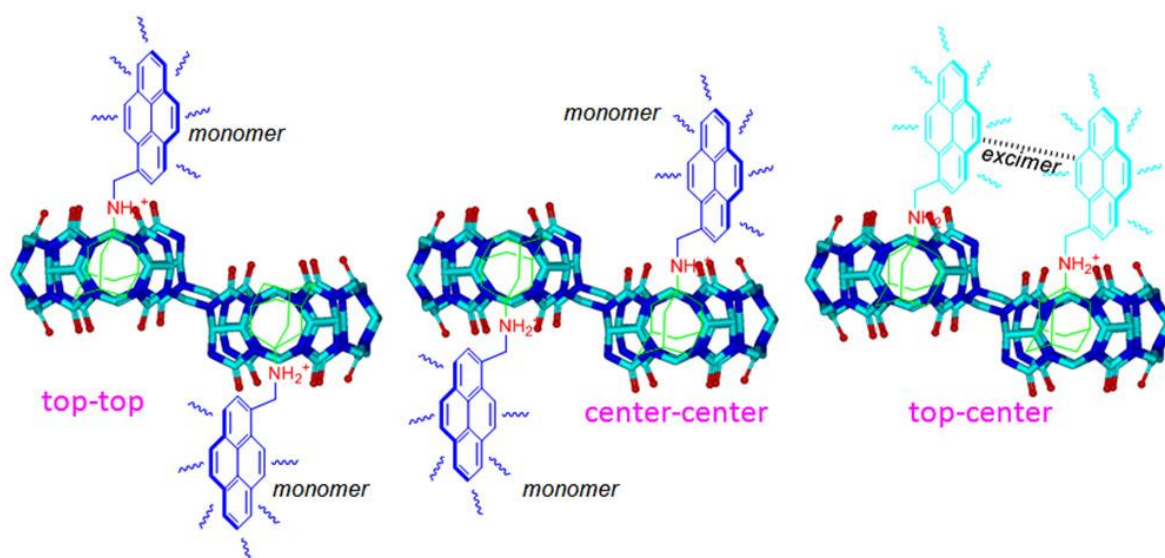
Figure 2 ^1H NMR spectra of G1 (1.0 mmol, D_2O , $\text{pD} = 2.0$) in the presence of host-2 at different concentrations at 298K.

In the case of the ^1H NMR titration experiments for host–guest interactions of G1–host-2, the chemical shift changes in G1 with increasing host-2 concentration are similar to those observed in the host-1 systems. However, the largest difference in the host–guest interaction properties between G1–host-2 and G1–host-1 is that the proton peaks on the benzyl group of G1 undergoes a large upfield shift (from δ 7.44 ppm to 6.75 and 6.37 ppm), as well as a slight proton downfield shift of the ADA moiety in the presence of host-2 (Figure 2). These spectral changes suggest that G1 accommodated its benzyl group into the cavities and that the ADA moiety remained in the portal of host-2, forming ternary complexes. These findings are also consistent with the behaviors observed by Isaacs and coworkers. That is, the bridging imidazolidone units of host-2 rigidify the structure of host-1, which has the ability to expand its cavity to accommodate larger guests. This effect makes it selective toward small guests [12].

As mentioned previously, Isaacs and coworkers reported their pioneering work on the host–guest interaction properties of host-1 and -2. Several diastereomers of some guests such as ADA were observed within ternary complexes of host-1 by ^1H NMR spectroscopy [9]. However, when we appended the benzyl group to the ADA moiety (G1) in the present study, the ^1H NMR spectra cannot provide the related

proton signals that distinguish the possible diastereomers of G1 in host-1 and -2, despite the clear split of resonances corresponding to the protons on the hosts .

A number of studies suggest that pyrene, is one of the most useful fluorogenic units, being sensitive to conformational change because of its relatively efficient monomer and excimer emissions [14]. For example, when pyrene instead of the benzyl group was appended to the ADA moiety (G2) in the present work, the top-center diastereomers of ADA-based derivatives within the host cavities could be distinguished by the novel photophysical property of pyrene (Scheme 2).



Scheme 2 Plausible diastereomers showing the fluorescence response of G2 with host-1.

Figure 3a shows changes in the fluorescence emission spectra of G2 in the presence of host-1. As can be seen, free G2 produced typical monomer emissions at around 378 and 396 nm in aqueous solution (pH=2) upon excitation of the pyrene fluorophore at 340 nm. When we added host-1 at increasing concentrations to the G1 solution, the fluorescence intensity of the G1 monomer emissions gradually decreased, while the maximum emission intensity at around 485 nm (typical excimer emissions of pyrene) increased. The excimer emission band of G2 can be attributed to the interaction of two pyrene units resulting in intermolecular π - π stacking, which was due to the two identical cavities of host-1. Consequently, the top-center isomerism of the G2-host-1 ternary complexes was conveniently confirmed from the optical signal after the changes in monomer/excimer fluorescence emissions of the pyrene groups on G2. Surprisingly, the fluorescence spectral changes of G2

(Figure 3b) suggest that a similar host–guest interaction triggered monomer-to-excimer binding response between G2 and host-2, similar to host-1 with G2, when we attempted to add host-2 to the G2 solution under the same conditions.

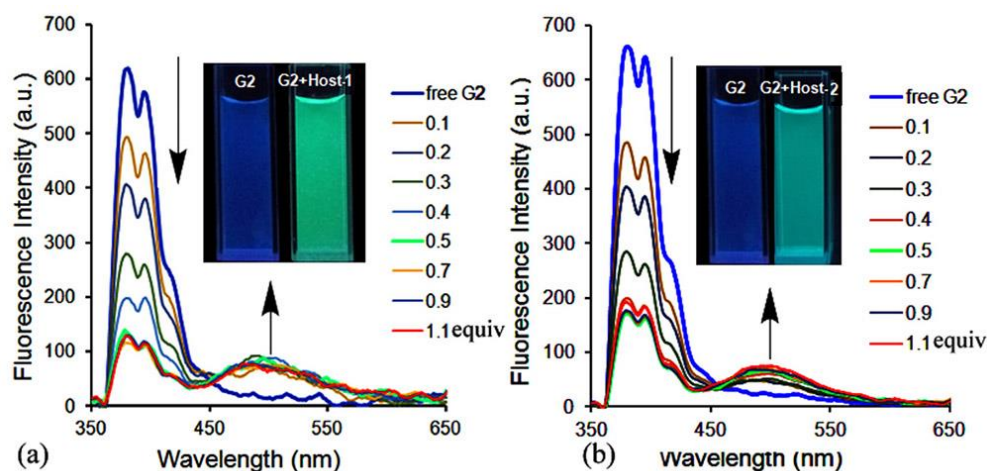


Figure 3 Fluorescence spectral changes of G2 (10.0 μM) in the presence of host-1 (a) and host-2 (b) at different concentrations in aqueous solution (pH 2.0) at 298K.

In order to obtain detailed information on the mechanism of the complexation of G2 with host-1 and 2, ^1H NMR titration experiments in aqueous solution were carried out. The spectral differences are shown in Figures. S1-S2. Upon addition of 0.5 equiv of host-1 to the solution of G2, the chemical shift of some protons on the ADA moiety shifted upfield because of the cavity's encapsulation of host-1, as expected. No significant chemical shift changes of the protons on pyrene moiety were observed. Importantly, the ^1H NMR spectral changes indicate that the rigid cavities of host-2 can accommodate the ADA moiety of G2. The upfield shift of protons on the ADA moiety can be observed despite the fast formation of a precipitate upon the addition of host-2 to a G2 solution. This result is very different from our previous observations on the host–guest interactions of G1 with host-2 and those of a study on ADA with host-2 by Isaacs and coworkers. In both cases, the ADA moiety was always rejected by the cavity of host-2.

Table 1. Thermodynamic binding data for G1·host-1, G2·host-1, G1·host-2, and G2·host-2 (Error = $\pm 10\%$).

Guest-Host	K_a (L·mol ⁻¹)	ΔG (kJ·mol ⁻¹)	ΔH (kJ·mol ⁻¹)	$T\Delta S$ (kJ·mol ⁻¹)
G1·host-1	1.32×10^5	-29.24	-50.90	-21.66
G2·host-1	7.64×10^6	-39.3	-65.77	-26.46
G1·host-2	4.51×10^6	-37.99	-39.01	-1.02
G2·host-2	1.08×10^7	-40.42	-30.96	9.46

Generally, the recognition binding ability for Q[n]s in aqueous solution is mainly due to the attraction between Q[n] hosts and guest based on the size or shape complementarily. This ability is aided by ion–dipole and dipole–dipole interactions arising from the electron-rich carbonyl rims of Q[n]s, the nonclassical hydrophobic effect of Q[n]s, and the classical hydrophobic effect of the guest [15]. The desolvation of the Q[n] host cavity releases high-energy water trapped in the cavity; this is a nonclassical hydrophobic effect because it has a favorable enthalpic signature. In contrast, the desolvation of the guest molecules is a classical hydrophobic effect; it possesses a favorable entropic component because of the release of surface-bound solvent molecules on the guest. Therefore, isothermal titration calorimetry could be employed to quantify the enthalpic and entropic contributions to the binding interactions between the hosts and guests (results are shown in Table 1 and Figures. S3-S4). The obtained thermodynamic parameters suggest that the ternary host–guest interactions of host-1 with G1 and G2, host-2 with G1 are almost exclusively enthalpy-driven ($\Delta H^\circ = -50.90$ kJ·mol⁻¹ and $T\Delta S^\circ = -21.66$ kJ·mol⁻¹ for inclusion complex G1·host-1; $\Delta H^\circ = -65.77$ kJ·mol⁻¹ and $T\Delta S^\circ = -26.46$ kJ·mol⁻¹ for the inclusion complex G2·host-1; $\Delta H^\circ = -39.01$ kJ·mol⁻¹ and $T\Delta S^\circ = -1.02$ kJ·mol⁻¹ for the inclusion complex G1·host-2); while only the formation of the inclusion complexes of host-2 with G2 is driven by both enthalpy and entropy ($\Delta H^\circ = -30.96$ kJ·mol⁻¹ and $T\Delta S^\circ = 9.46$ kJ·mol⁻¹). Evidently, the high enthalpy gain for host-1 with G1 and G2, host-2 with G1 may be attributed to the strong ion–dipole interactions between the guest and host. However, the host–guest interactions in the case of complexes of G2·host-2 are derived not only from the ion–dipole interactions between the host and guest, but also in the assistant of the hydrophobic effect. Notably, the entropic gain achieved with the G2·host-2 system was higher than that obtained with other host-

guest systems, indicating that the large hydrophobic side group pyrene is enabling the classical hydrophobic effect in aqueous solution as the guest indeed. On the other hand, the thermodynamic parameters obtained in the present study also suggest that the rigidify cavity structure such as host-**2** is benefit for the classical hydrophobic effect of guest in aqueous solution.

Conclusion

In summary, we evaluated the molecular recognition triggered by a novel host–guest interaction of NS-CB[10]-based host-**1** and -**2**. The unique monomer and excimer fluorescence emissions of pyrene due to the two-cavities of the host–guest system were exploited to identify the possible diastereomers. The top–center isomerism of the ternary complexes of **G2** with the hosts was eventually identified from the distinct photophysical signals of pyrene. Interestingly, we found that being a large hydrophobic side group on the guests, pyrene plays important roles in improving the guest recognition and the binding ability of the hosts. This study showed that gradually tuning the side groups of the guest molecules from hydrophilic to hydrophobic may provide new insights into the dependence of molecular recognition on the host cavity size in aqueous solution.

Supporting Information

Supporting Information File 1:

Title: Experimental data, additional ¹H NMR spectra and others.

Acknowledgements

This work was supported by the National Natural Science Foundation of China (21361006), the Science and Technology Talent Fund of Guizhou Province (20165656), and the Graduate Student's Fund for innovation of Guizhou University (2017008).

References

- 1 Changeux, J. P.; Edelman, S. *F1000 Biol. Rep.* **2011**, 3
- 2 Day, A. I.; Arnold, A. P.; Blanch, R. J.; Snushall, B. *J. Org. Chem.* **2001**, 66, 8094–8100.
- 3 Kim, J.; Jung, I. S.; Kim, S.Y.; Lee, E.; Kang, J. K.; Sakamoto, S.; Yamaguchi, K.; Kim, K. *J. Am. Chem. Soc.* **2000**, 122, 540–541.
- 4 (a) Barrow, S. J.; Kasera, S.; Rowland, M. J.; Barrio, J. D.; Scherman, O. A. *Chem. Rev.* **2015**, 115, 12320–12406; (b) X. L. Ni, X. Xiao, H. Cong, Q. J. Zhu, S. F. Xue and Z. Tao, *Acc. Chem. Res.* **2014**, 47, 1386–1395; (c) A. C. Bhasikuttan, H. Pal and J. Mohanty, *Chem. Commun.* **2011**, 47, 9959–9971; (d) Yang, X.; Liu, F.; Zhao, Z.; Liang, F.; Zhang, H.; Liu, S. *Chin. Chem. Lett.* **2018**, 29, 1560–1566.
- 5 (a) Jiao, Y.; Li, W. L.; Xu, J. F.; Wang, G.; Li, J.; Wang, Z.; Zhang, X. *Angew. Chem., Int. Ed.* 2016, **55**, 8933–8937; (b) Cui, X.; Zhao, W.; Chen, K.; Ni, X. L.; Zhang, Y. Q.; Tao, Z. *Chem. Eur. J.* **2017**, 23, 2759–2763; (c) Zhang, Q.; Wang, W. Z.; Yu, J. J.; Qu, D. H.; Tian, H. *Adv. Mater.* **2017**, 29, 1604948; (d) Gong, W. J.; Yang, X. R.; Zavalij, Y.; Isaacs, L.; Zhao, Z. Y.; Liu, S. M. *Chem. Eur. J.* **2016**, 22, 17612–17618; (e) Mao, D.; Liang, Y.; Liu, Y.; Zhou, X.; Ma, J.; Jiang, B.; Liu, J.; Ma, D. *Angew. Chem., Int. Ed.* **2017**, 56, 12614–12618; (f) Wu, W.; Song, S.; Cui, X.; Sun, T.; Zhang, J.-X.; Ni, X.-L. *Chin. Chem. Lett.* **2018**, 29, 95–98.
- 6 (a) Kim, H. J.; Heo, J.; Jeon, W. S.; Lee, E.; Kim, J.; Sakamoto, S.; Yamaguchi, K.; Kim, K. *Angew. Chem., Int. Ed.* **2001**, 40, 1526–1529; (b) Ko, Y. H.; Kim, E.; Hwang, I.; Kim, K. *Chem. Commun.* **2007**, 1305–1315.
- 7 (a) Wang, X. Q.; Lei, Q.; Zhu, J. Y.; Wang, W. J.; Cheng, Q.; Gao, F.; Sun, Y. X.; Zhang, X. Z. *ACS Appl. Mater. Interfaces* **2016**, 8, 22892–22899; (b) Li, S.; Jiang, N.; Zhao, W.; Ding, Y.-F.; Zheng, Y.; Wang, L.-H.; Zheng, J.; Wang, R. *Chem. Commun.* **2017**, 53, 5870–5873.
- 8 (a) Liu, Y. L.; Yang, H.; Wang, Z. Q.; Zhang, X.; *Chem. Asian J.* **2013**, 8, 1626–1632; (b) Tian, J.; Chen, L.; Zhang, D.-W.; Liu, Y.; Li, Z.-T. *Chem. Commun.* **2016**, 52, 6351–6362; (c) Ni, X. L.; Chen, S.; Yang, Y.; Tao, Z. *J. Am. Chem. Soc.* **2016**, 138, 6177–6183; (d) Y. Xia, S. Chen and X.-L. Ni, ACS

- Appl. Mater. Interfaces* **2018**, *10*, 13048–13052; (e) Wu, H.; Chen, Y.; Dai, X.; Li, P.; Stoddart, J. F.; Y. Liu, *J. Am. Chem. Soc.* **2019**, *141*, 6583–6591.
- 9 Huang, W. H.; Liu, S.; Zavalij, P. Y.; Isaacs, L. *J. Am. Chem. Soc.* **2006**, *128*, 14744–14755.
- 10 (a) Nally, R.; Scherman, O. A.; Isaacs, L. *Supramol. Chem.* **2010**, *22*, 683–690; (b) Nally, R.; Isaacs, L. *Tetrahedron*, **2009**, *65*, 7249–7258; (c) Park, K. M.; Roh, J. H.; Sung, G.; Murray, J.; Kim, K. *Chem. Asian J.* **2017**, *12*, 1461–1464.
- 11 Appel, E. A.; Barrio, J. D.; Dyson, J.; Isaacs, L.; Scherman, O. A. *Chem. Sci.* **2012**, *3*, 2278–2281.
- 12 Wittenberg, J. B.; Costales, M. G.; Zavalij, P. Y.; Isaacs, L. *Chem. Commun.* **2011**, *47*, 9420–9422.
- 13 Liu, S.; Ruspic, C.; Mukhopadhyay, P.; Chakrabarti, S.; Zavalij, P. Y.; Isaacs, L. *J. Am. Chem. Soc.* **2005**, *127*, 15959–15967.
- 14 Kim, J.; Quang, D. T. *Chem. Rev.*, **2007**, *107*, 3780–3799.
- 15 (a) Biedermann, F.; Uzunova, V. D.; Scherman, O. A.; Nau, W. M.; De Simone, A. *J. Am. Chem. Soc.* **2012**, *134*, 15318–15323; (b) Biedermann, F.; Vendruscolo, M.; Scherman, O. A.; A. De Simone and W. M. Nau, *J. Am. Chem. Soc.* **2013**, *135*, 14879–14888; (c) Huang, Z.; Qin, K.; Deng, G.; Wu, G.; Bai, Y.; Xu, J.-F.; Wang, Z.; Yu, Z.; Scherman, O. A.; Zhang, X. *Langmuir* **2016**, *32*, 12352–12360.